Optical coherence tomography angiography measures blood pulsatile waveforms at variable tissue depths

Zhiying Xie, Geng Wang, Yuxuan Cheng, Qinqin Zhang, Minh Nhan Le, Ruikang K. Wang

Department of Bioengineering, University of Washington, Seattle, WA, USA

Correspondence to: Ruikang K. Wang. Department of Bioengineering, University of Washington, Seattle, WA, USA. Email: wangrk@uw.edu.

Background: Photoplethysmography (PPG) is routinely used to detect the blood pulse signal from skin tissue beds in clinics. However, the origin of the PPG signal remains controversial. The purpose of this study is to explore optical coherence tomography angiography (OCTA) to indicate pulsatile waveforms in the papillary plexus and dermal plexus separately under different hand elevations.

Method: Optical microangiography (OMAG) algorithm was used to obtain a 3D OCTA signals, from which the depth-resolved pulsatile blood flow signals were extracted from different skin vascular plexus. The systolic amplitude, crest time, and delta T were measured from the OCTA pulsatile signals when the hand was placed at the positions of 50 cm below, 0 cm, and 50 cm above the heart level.

Results: The pulse signal integrated from all the depths has a similar waveform to that of the PPG and showed the same morphological change at different hand elevations. The pulsatile patterns from the papillary plexus and dermal plexus showed distinct morphological changes at different local blood pressure. Less amplitude difference was found from papillary plexus comparing to that of the dermal plexus. Crest time was found in an increasing trend in the OCTA pulsatile waveform from both plexuses when the arm was raised from the position below to above the heart level. In contrast, a decreasing trend of Delta T was detected in the dermal pulsatile but was not observed from that of the papillary plexus, indicating that vascular resistance associated with the arm elevations does not necessarily have the same effect on the two plexuses.

Conclusions: OCTA can provide depth-resolved pulsatile waveforms within different microvascular plexus within tissue skin beds. This technique could open doors to understanding the mechanisms of how blood flow changes at different skin circulatory plexus.

Keywords: Pulsatile waveform, Photoplethysmography (PPG), Optical Microangiography (OMAG), Optical coherence tomography angiography (OCTA)

Introduction

Photoplethysmography (PPG) is a non-invasive optical technique that is often used to measure the pulsatility of cutaneous blood flow by detecting subtle variations in tissue blood volume through light absorption (1). PPG signal is composed of a slowly varying DC signal associated with non-pulsatile blood, tissue and bone, and a pulsatile AC waveform that is related to the increase/decrease of blood volume within tissue beds due to each heartbeat. The AC component of the waveform rises during the systolic phase and falls during the diastolic phase, periodically following the same trend as the blood volume change during systolic and diastolic phases of each heartbeat.

PPG signal could be interpreted as a summation of the forward propagation wave generated by vessel contraction and the backward reflective wave generated by vessel relaxation from the periphery (2). The backward reflective wave is induced as blood travels through the vascular tree and being reflected by the bifurcated vessels or the elastic

arterial vessel walls. As pulsatile blood propagates from the central arteries to the periphery vessels, the increased resistance in peripheral vessels would induce more reflection waves. The alternation in the PPG waveform has been reported to associate with aging or disease processes such as hypertension, diabetes, atherosclerosis, and large vessel stiffening (1,3,4). Although extensive research and application of PPG have shown potential in evaluating the cardiovascular system (5-8), hitherto, the origin of the PPG waveform, however, remains elusive and controversial in terms of whether the signal is from superficial capillary beds, arterioles in relatively deeper dermal layers, or simply from background tissue compositions where the change in optical property may be modulated by the blood volume changes within tissue beds.

Optical coherence tomography (OCT) based angiography (OCTA) has demonstrated the capability to visualize cutaneous blood flow with depth-resolved information and in high resolution (9-15). Blood flow information can be isolated from the static tissue utilizing a motion contrast algorithm, optical microangiography (OMAG), based on an eigen decomposition (ED) approach (15-17). The high imaging resolution from OCT allows the technique to distinguish small blood vessels within capillary beds from relatively large blood vessels at deeper depth locations. The light source of the OCT system is operated at near-infrared wavelength, which is similar to the typical 940 nm PPG light source giving a similar penetration depth and functionality. In particular, ED-OMAG contrasts the moving blood flow with a signal strength proportional to the blood cell flux, i.e., the volume of red blood cells passing through vessel cross-section per unit area (18,19). Volumetric flux is in proportion to the volume change and is suggested to be affected by similar vascular mechanisms (20). Therefore, it would be reasonable to compare the pulsatile blood flows measured by the two technologies. Moreover, benefiting from the depth-resolved imaging, OCTA has the capability to separate pulsatile information from different cutaneous circulatory plexuses. Thus, this capability would provide us with an opportunity to extract and compare the property of blood flow pulsations from both the papillary and dermal plexuses simultaneously.

In this paper, we report a new method that uses the OCTA signals to provide reliable depth-resolved pulsatile blood waveforms within tissue beds. It was suggested that the PPG signal might be associated with arteriole blood pressure not only due to its similarity in waveform but also because of its proportional relationship between arterial blood pressure and blood volume (7,21). Similar to the strategy used in PPG studies (22-25), we have conducted a hand-raising experiment to understand better how local blood pressure and peripheral resistance affects the morphology of pulse waveforms in the different cutaneous circulatory plexuses. The force of gravity could significantly alter local blood pressure and peripheral blood flow resistance due to cutaneous vessel autoregulation adjustment (22). When the hand is below the heart level, the increased capillary pressure will induce vasoconstriction of the arterioles, resulting in increased pre-capillary flow resistance and decreased post-capillary flow resistance. Conversely, when the hand is elevated, the decreased capillary pressure would induce arteriole to dilate, resulting in a decrease of pre-capillary flow resistance and increase of post-capillary flow resistance (26). Such a simple experimental strategy has been utilized by various research groups when developing PPG, Camera-based PPG, laser doppler flowmetry, etc. (23-27) to test the validity of the measurements by examining the change in flow resistance at different blood pressures. However, no technique is currently available that is able to observe the pulsatile waveform from circulatory plexuses at specific tissue depths separately under the effect of hand elevation because currently available technique does not provide depth resolved information. Thus, this study could provide valuable clues for understanding the mechanical property of how blood travels through different types of vasculature networks under the effect of flow resistance and elucidate its potential applications in disease assessments.

Methods

The OCTA pulsatile signals were measured in five young, healthy volunteers (n=5; 3 males, 2 females). We used a hand-held swept-source OCT (SS-OCT) system (28) to collect OCTA signals from fingers in human subjects to represent pulsatile blood waveforms within skin tissue beds. This system employed a 200 kHz swept light source operated at a central wavelength of 1,310 nm and a spectral bandwidth of 100 nm, providing ~8 μm axial resolution. A laboratory-built transmission mode PPG device was also used to collect the PPG signals from the finger to indicate blood volume changes for reference. The imaging of subjects reported in this study using a laboratory-built investigational device was conducted in accordance with a protocol approved by the Institutional Review Board of the University of Washington, and informed consent was obtained from all subjects. The
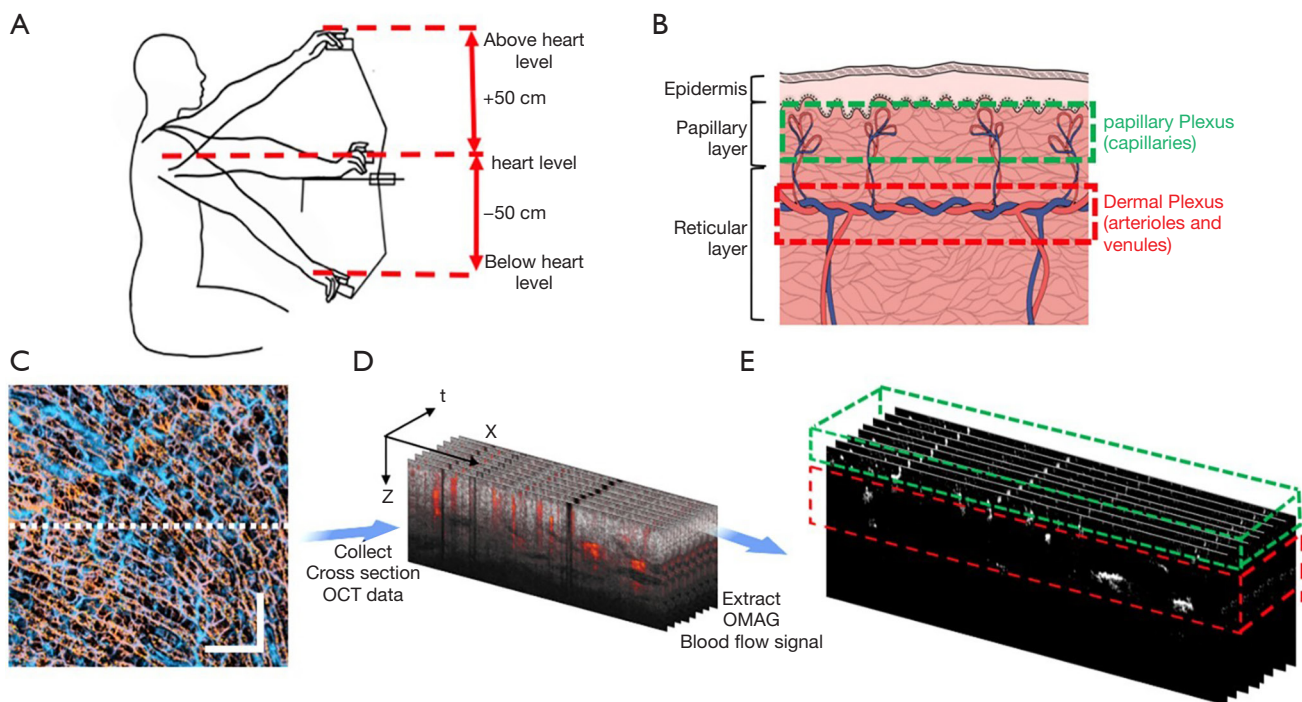
Figure 1 Schematic of the experimental design. (A) The set-up of the collection procedure at different hand elevations. The heights of the hand relative to the heart were +50, 0, –50 cm, respectively. (B) The relationship between the papillary plexus (capillary bed) and the dermal plexus (arteriole and venous). (C) Representative 3D OCTA microvascular image color-coded by depth information, where orange indicates the papillary capillary vessel networks and blue, indicates the dermal plexus. The scale bar = 0.5 mm. (D) Time series of repeated OCT B-scans at the position shown as a dashed line in (C), from which (E) OCTA blood flow signals were extracted. The green dotted box is an illustration of the tissue layer that contains the papillary plexus. The red dotted box is an illustration of the tissue layer that contains the dermal plexus.

study followed the tenets of the Declaration of Helsinki and was conducted in compliance with the Health Insurance Portability and Accountability Act.

In this study, OCT datasets were acquired on the index finger at three different hand elevation: above (+50 cm), same (0 cm), and below (–50 cm) heart level (*Figure 1*). The data was collected in a sitting position, with regular breathing and minimal body movement. The OCT hand-held probe was placed on an adjustable hand rest. The height of the chair was adjusted so that the hand could be leveled with the vertical mid-point of the sternum when placed on the probe, which was approximately the level of the heart. The probe could be adjusted to allow the hand placed below or above the heart level, or to form a 45-degree angle between the trunk and arm to avoid building unnecessary tension or stress on the arm. PPG signal was collected from the middle finger on the same

hand. We avoided measurement sites that may contain large arteries and asked the volunteer to keep the finger still with minimal pressure applied to the detector to eliminate motion artifacts caused by tissue deformation. Before data collection, the volunteers were asked to rest for at least 5 minutes to accommodate the environment. Measurements were captured in a quiet and controlled room temperature environment at the same hour each day.

Two scanning protocols were designed in this study. The first protocol was designed to provide 3D OCT structural and OCTA blood flow images of scanned tissue volume, in which the scans contained 1,000×5 B-frames (i.e., 1,000 scan locations with each position having five repeated B-scans), and each B-frame was composed of 1,000 A-scans. The field of view was 2.5×2.5 mm^2. The resulted 3D images (*Figure 1C*) were used to guide the depth selection of the cutaneous plexus for the extraction
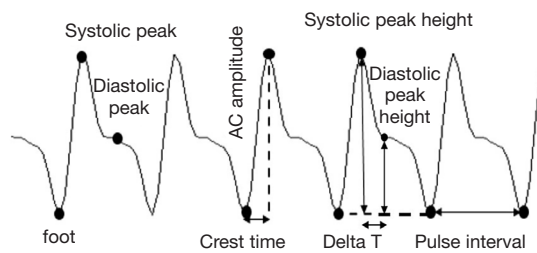
Figure 2 Morphology parameters used to assess the pulse waveforms in this study.

of pulse waveforms. Since the cutaneous vessels consist of horizontal microvascular networks with interweaved arteriole and venules from which the nutritive capillary bed arises, the two plexuses can be separated based on their relative depth and vessel structure from the 3D microvasculature image (*Figure 1B,E*) (29).

The second protocol was designed to extract pulsatile waveforms from OCTA signals, in which 4,000 repeated B-scans were continuously collected at one same position over a period of ~10 s (*Figure 1D*). The B-scan consisted of 300 A-scans (covering 1.0 mm), which led to an imaging rate at 400 frames per second, providing sufficient temporal resolution to observe pulsatile blood flow signals.

All signals were processed and analyzed retrospectively in MATLAB (The MathWorks, Inc., USA). 3D OCTA blood flow image was generated by the OMAG algorithm using an eigen decomposition (ED) approach (*Figure 1C*). OMAG contrasts the movement of blood flow from the static tissues by comparing 5 repeated B-frames. The well-known projection artifacts within OCTA blood flow images were removed using an algorithm previously published in (30,31). From the 3D OCTA images, we identified approximate depths for proper segmentation of papillary capillary plexus (~100 to 300 μm from the skin surface) and dermal plexus (~300 to 1,500 μm from the skin surface) for the time series of B-scans to evaluate the pulse waveforms (*Figure 1E*).

Time series of OCTA blood flow images were generated by the complex OMAG algorithm (15) using the repeated B-scans (*Figure 1D*). Five consecutive B-scans was used to obtain one OCTA B-scan blood flow image. We assumed the pulse signal from the papillary dermis layer was from the capillary bed, and the pulse signals from the dermal plexus were primarily from the arterioles where the pulsation in the venules could be omitted (32). The pulse signal from each microvascular plexus was obtained by integrating the

intensity signals, *I(t)*, within the region of interest from the temporal OCTA blood flow images, *OCTA(x,y,t)*, and was plotted in a temporal relationship.

$$I(t) = \iint OCTA(x, y, t)dxdy \qquad [1]$$

Where *x* and *y* indicate the pixel indices in the OCTA image. The pulse signal was also measured by integrating the OCTA signals from both plexuses (papillary plexus and dermal plexus). The obtained time-varying signal was then passed through a designed bandpass finite-duration impulse response (FIR) Equiripple filter (0.7–10 Hz) with 40 dB attenuation in the stopbands, to obtain the final pulse waveform.

The repeatability of the measured pulse waveforms was assessed by calculating their coefficients of variance. In this test, we conducted five imaging sessions at the same skin position to each collect 10-second temporal OCTA scans where each imaging session was resumed by re-positioning the finger under the OCT probe after the prior session. The resulted pulse waveforms were analyzed for their amplitude and peak to peak interval to demonstrate the repeatability of the technique.

To characterize the OCTA pulsatile waveforms, we followed the convention that is often used in the field of PPG (*Figure 2*). The systolic peaks of each pulsatile waveform were found by an adaptive peak finder algorithm implemented in MATLAB (Findpeaks). The systolic foot and diastolic peaks were obtained by the local maximum of the second derivatives. Three parameters (AC amplitude, crest time, and delta T) were measured from the OCTA pulsatile waveform for the assessment of its morphology (*Figure 2*). The AC amplitude was measured by the difference in amplitude between the systolic peak and foot of the waveform. Crest time was measured by the time interval between the foot and systolic peak. This parameter indicates the flow resistance in the forward wave. Delta T was measured by the time interval between the systolic and diastolic peaks. It is associated with relationship between the forward and reflected waves, which often indicates the peripheral flow resistance. For ease comparison, the AC amplitude from all plexus was normalized to the geometric mean of the AC amplitudes from all plexus pulsatile measured at heart level. The AC amplitude from papillary and dermal plexus was normalized to the geometric mean of the AC amplitudes from the dermal plexus at the heart level. The time differences in the morphological values were normalized to the pulse interval of each heartbeat accordingly to eliminate individual differences.
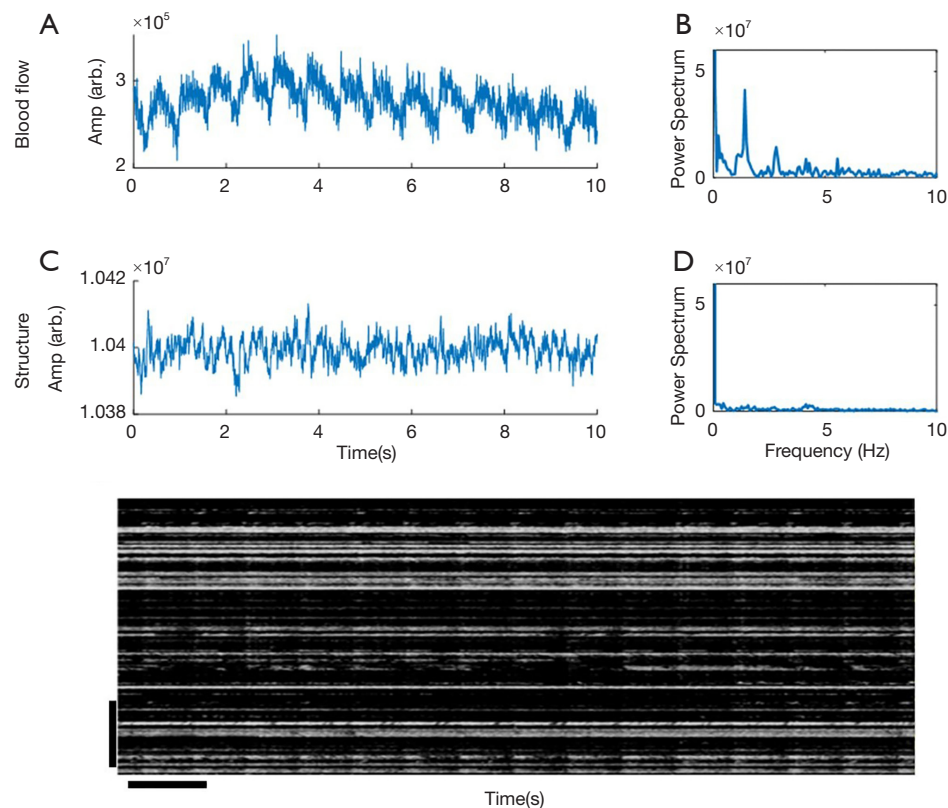
Figure 3 Illustration of intensity signal and power spectrum from the OCT structure and OCTA blood flow signals. The temporal intensity signals obtained from (A) OCTA blood flow image, and (C) the OCT structural image, respectively. The spectra in (B) and (D) show the frequency power of (A) and (C) correspondingly (FFT). (E) temporal image extracted from 10-sec repeated B-scans, showing the consistent changes in blood volume of all vessel plexus corresponding to each heartbeat. The image shown is the maximum projection image that was projected from both the papillary and dermal plexus (see in *Figure 1E*). The scale bar in the left =500 µm, and that in the bottom left = 1 second.

To compare the change in morphologies related to the hand positions, the geometric mean of the morphological variables, and the 95% confidence interval (±95% CI) was calculated. A one-way ANOVA was used to test for the significance of the difference in mean of the morphological values measured from all plexus. Two-way ANOVA was used to test for the significance of the difference in the mean of the morphological values measured from the papillary plexus and dermal plexus.

Results

Figure 3 shows the representative time series of OCTA blood flow and OCT structural signals from the index finger at the heart level (h =0 cm). In this example, the OCTA blood flow intensity signals (*Figure 3A,B*) showed

cycling periods at 1.4 Hz that matched well with that measured by a heart rate monitor. Strong spectral power was observed at the harmonic frequencies produced by Fourier transformation, which usually contains the most biological signals (*Figure 3B*). Much weaker periodical signal was found in the OCT structural signal, which included signals from the blood flow and static tissues (*Figure 3C,D*). The change in temporal intensity signals from the OCTA image (*Figure 3E*) indicates that blood flow in all the vessels spikes with each heartbeat and gradually decays. The repeatability study showed that the coefficients of variance of the amplitude and pulse interval were around 5%, demonstrating that the OCTA measurement of blood pulse signals is repeatable (*Table 1*).

Figure 4 illustrates the morphological difference of the representative OCTA pulsatile signals from all plexus (i.e.,

the integration of all blood flow signals) comparing to PPG pulsatile signals at three hand elevations. It is observed that the diastolic peak was more noticeable when the hand was below the heart level and was less distinguishable from the systolic peak when the hand was above the heart level, consistent with the previous observations described by the PPG measurement (24).
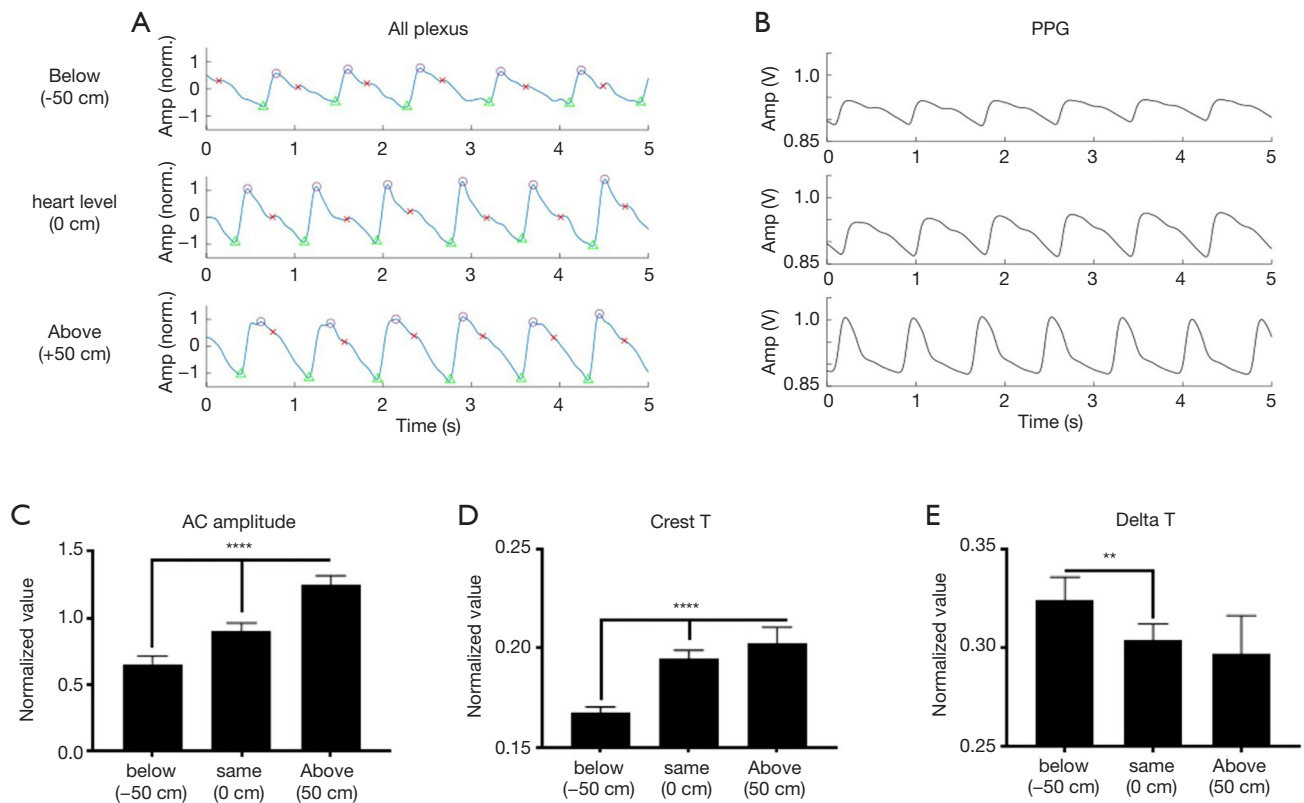
The normalized mean AC amplitude of the pulsatile waveform in all plexus changed in conformity with the position of the hand relative to the heart (*Figure 4C*).

Mean AC pulsation was the lowest when the hand was below the heart (h = −50 cm) and showed a trend of increase as the hand elevated. Normalized mean crest time and delta T were found significantly different at different hand positions relative to the heart (*Figure 4D*). Crest time showed an increasing trend, and delta T showed a decreasing trend when the hand was raised from below heart level (h = −50 cm) to above heart level (h = +50 cm). These observations are consistent with the results observed in the PPG study (24).

Figure 5 demonstrates the differences in morphology of the pulsatile waveforms from the papillary plexus (*Figure 5A*) and dermal plexus (*Figure 5B*) at different hand elevations. Similar to the results observed from all plexus (*Figure 4*), AC pulsation in dermal plexus showed an increasing trend when the hand was changed to an elevated position (*Figure 5C*). AC pulsation was the greatest in the papillary plexus when the hand was at the heart level, whereas it was decreased when the hand was

Table 1 Coefficient of variation (CV) of the pulse transit time and heart rate calculated from the processed waveform

	Pulsatile amplitude (CV), %	Peak to peak interval (CV), %
Papillary	3.22	4.71
Dermal	1.34	5.00
All plexus	1.47	5.09

Figure 4 Five-second demonstration of the pulsatile waveform from all plexus collected by (A) OCTA and (B) PPG when the hand is below heart level (−50 cm), at heart level (0 cm), and above heart level (+50 cm). (C,D,E) Geometric mean (±95% CI) of the morphological variables of AC amplitude (C), crest time (D) and delta T (E) from the OCTA pulsatile waveform form. **, P<0.001; ****, P<0.0001.
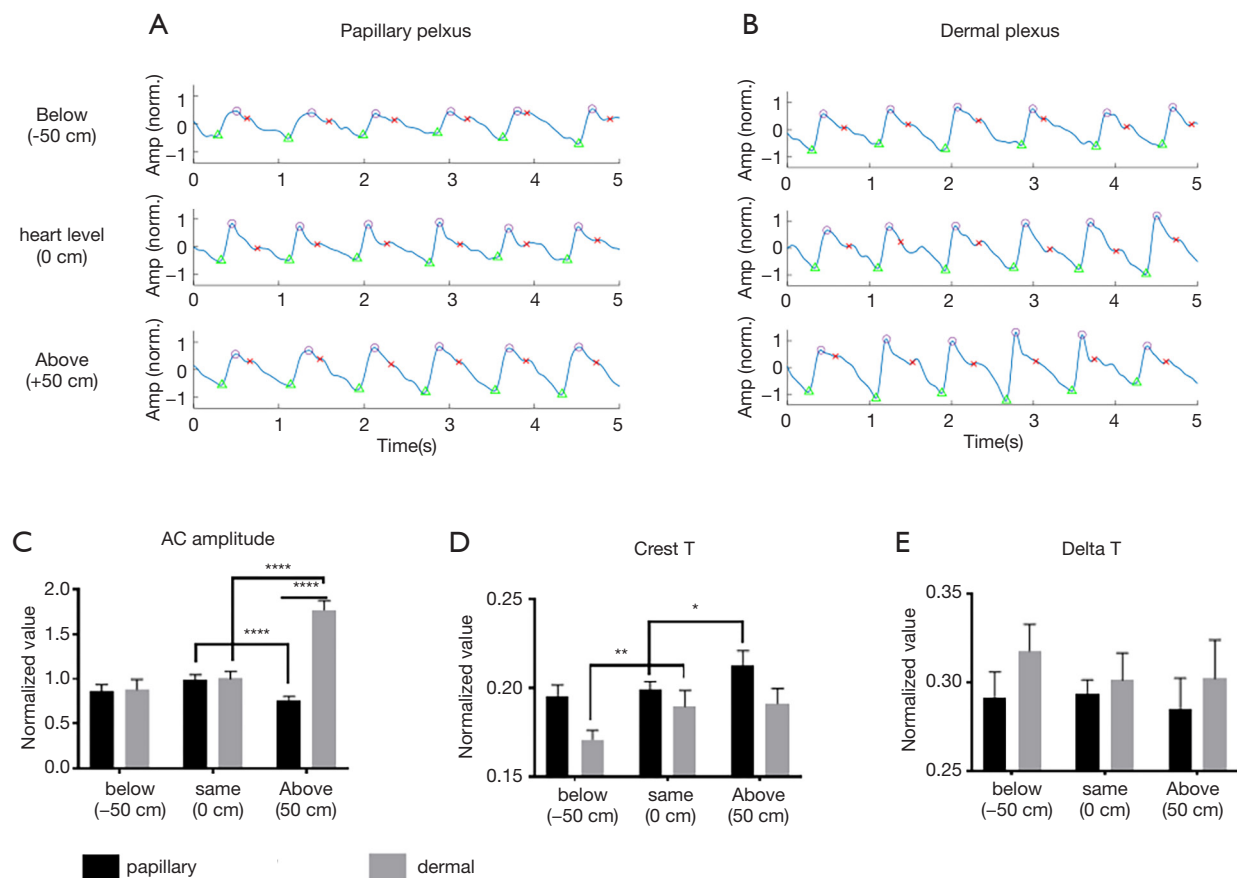
Figure 5 Five-second demonstration of the pulsatile waveform from (A) the papillary plexus, and (B) dermal plexus when the hand is below heart level (–50 cm), at heart level (0 cm), and above heart level (+50 cm). (C,D,E) Geometric mean (±95% CI) of the morphological variables of AC amplitude (C), crest time (D) and delta T (E) from the OCTA pulsatile waveform form from each plexus. *, $P<0.05$; **, $P<0.001$; ****, $P<0.0001$.

above or below the heart level. A significant difference in AC pulsation was found between the dermal and papillary pulsatile when the hand was above the heart level ($h = +50$ cm), whereas no difference was found in the AC pulsation between the papillary plexus and dermal plexus when the hand was at heart level and below heart level (*Figure 5C*). Approximately, a two-fold difference was found in the AC pulsation from the dermal plexus compared to that of papillary plexus. A longer crest time was observed in both papillary and dermal pulsatile when the hand was elevated (*Figure 5D*), similar to that of all plexus. Dermal pulsatility showed a decreased trend in delta T as the hand was raised to above the heart level (*Figure 5E*). No difference in delta T was observed in the papillary pulsatility at different hand elevations.

Discussion

In this study, pulsatile signals in the cutaneous circulatory system were successfully extracted with the support of OCTA through an eigen-decomposition based OMAG approach. The results demonstrated the potential of how OCTA could become a reliable, non-invasive imaging tool measuring the pulsatile waveforms. Although PPG detects the changes based on the light absorption by blood volume, and OCTA detect the changes of the backscattering light due to the difference in the blood volume. We found that OCTA pulsatile waveform has similar morphological changes to the PPG signals at different hand elevations (24) since they are both describing the property of blood volume change between each heartbeat. The PPG AC signal relies

on the volumetric change in the cutaneous vessels. In contrast, OCTA gave a measurement that is proportional to the volumetric flux that is associated with the number of red blood cells passed through vessels. The volumetric flux change is driven by the same fluid dynamic mechanism of the source of the AC PPG signal.

Similar to the PPG results reported by Hickey *et al.* (24) we observed a consistent increase of the AC pulsation derived by integrating all OCTA signals across all plexuses when the hand was raised from below heart level to above heart level. The change of AC pulsation is associated with a change in pulsating blood volume in the cutaneous vessels due to the venoarterial reflex (VAR) (22,23,33). Autoregulation in the arterioles adjusts the blood vessel diameter in response to the disruption in blood flow and perfusion pressure in the venues. When the hand is above the heart level, the hydrostatic effect would cause the venous wall to collapse due to a drop in venous pressure. This effect may cause vasodilation in the arterioles, so that blood volume in the arteriole would increase. When the hand is below the heart level, venous vessels would distend, causing vasoconstriction in the arteriole.

AC pulsation from the papillary plexus and dermal plexus is regulated by the VAR at different hand elevations (22). But the AC pulsation across the plexus may have a distinct trend due to the difference in the vessel function and mechanical properties. However, due to the nature of its working principle, PPG is not able to track the change in the dermal plexus and papillary plexus separately (34).

Consistently, we observed the similar trend in the OCTA pulsatile directly measured from dermal plexus at changing hand elevations. In contrast, a distinct pattern was detected from papillary AC amplitude, which may be induced by the change in pre-capillary blood pressure. When the hand is at heart level and below heart level, the same volume of pulsating blood might be delivered across the plexuses indicated by the same AC amplitude observed from both plexuses. When the hand is above the heart level, reduced pre-capillary blood pressure may lead to a reduction of blood flow in the capillary vessels so that a decrease in AC pulsation is detected (22).

Crest time, which is the time difference between the foot of the pulsatile signal and the systolic peak, measures the time used for the rapid injection of blood during the systolic phase. Based on previous studies, an increase in crest time is associated with increased blood flow resistance, aging, or disease relative vascular changes

(35-37). Increased blood flow resistance would delay the systolic phase. The trend of increasing crest time from all plexus detected by both PPG and OCTA may indicate that there could be an increase in blood flow resistance as the hand changed from below heart level to above heart level. The same trend was observed in the OCTA pulsatile signal detected from both the papillary and dermal plexus, indicating that flow resistance has the same influence on both plexuses. When the hand is changed into an elevated position, vasoconstrictions in the arteriole may cause increased resistance resulted in an increasing trend in Crest time and vice versa (38). Capillary blood flow resistance is proportional to systemic hematocrit as red blood cells being pushed into the bifurcated small capillary vessels. Hand elevation may induce a drop in local blood pressure that induces flow resistance indicated by a decreased crest time.

When the incident pulse wave moves from the heart to the peripheral vessels, it would come across an impedance mismatch at vessel junctions and in small vessels that have high resistance (2). The impedance would influence the incoming blood flow generating a reflected pressure wave, which is observed as the diastolic peak. Delta T, which is the time interval between the systolic peak and diastolic peak, measures the time taken for the reflective wave from heart and back. The trend of decrease in Delta T may be associated with the increased vascular tone, and high pulse wave velocity occurred in the arteriole (24). Both PPG and OCTA pulsatile waveforms showed a decreasing trend in delta T as the hand was elevated above the heart. However, the same pattern was detected in the dermal pulsatile but was not observed from that of the papillary plexus, indicating that the vascular tone and wave velocity did not change in the capillary beds.

However, some morphology values were not significant when comparing under the condition of different hand elevations. Two factors may induce high variation or noise. First, the number of subjects tested in this study was limited. Even though geometric mean was used to indicate the central tendency of the set of values, an insufficient sample size would limit the potential to detect significant differences. A large cohort of subject study is warranted to increase the statistical power for the current study. Second, the intensity signal measured at different sites could be profoundly affected by local factors, including microvasculature density, local blood flow activity, skin melanin, epidermal thickness, and so on (39).

Conclusions

In conclusion, we have demonstrated that OCTA is capable of generating pulse waveforms of the blood volume change within the superficial skin tissue beds up to 1.5 mm in depth. OCTA pulsatile waveforms showed similar morphological trend to that of the PPG studies at three different hand elevations. Benefiting from the depth-resolved information, we have found that the trend of change in AC amplitude and delta T behaves differently in the papillary and dermal pulsatility. The pattern of pulsatile morphology change follows the physical properties of the VAR effect, which are due to vessel autoregulation adjustments, pre-capillary blood flow resistance and pressure, and peripheral blood vessel reflectance. This technique may open doors for understanding the mechanisms of how blood flow in different cutaneous plexuses responds to the VAR effect based on the changes in volumetric flux in blood vessels associated with the number of red blood cells. We expect that it could also be developed for blood pressure measurement, disease assessment, and risk stratification, or health condition of the individual's blood vessel or heart chamber indication.

Acknowledgments

Footnote

Provenance and Peer Review: With the arrangement by the Guest Editors and the editorial office, this article has been reviewed by external peers.

Conflicts of Interest: All authors have completed the ICMJE uniform disclosure form (available at http://dx.doi.org/10.21037/qims-20-778). The special issue "Advanced Optical Imaging in Biomedicine" was commissioned by the editorial office without any funding or sponsorship. RKW served as the unpaid Guest Editor of the special issue and serves as an unpaid Deputy Editor of *Quantitative Imaging in Medicine and Surgery*. The authors have no other conflicts of interest to declare.

Ethical Statement: The imaging of subjects reported in this study using a laboratory-built investigational device was conducted in accordance with a protocol approved by the Institutional Review Board of the University of Washington, and informed consent was obtained from all subjects. The study followed the tenets of the Declaration of Helsinki and was conducted in compliance with the Health Insurance Portability and Accountability Act.

Open Access Statement: This is an Open Access article distributed in accordance with the Creative Commons Attribution-NonCommercial-NoDerivs 4.0 International License (CC BY-NC-ND 4.0), which permits the non-commercial replication and distribution of the article with the strict proviso that no changes or edits are made and the original work is properly cited (including links to both the formal publication through the relevant DOI and the license). See: https://creativecommons.org/licenses/by-nc-nd/4.0/.

References

1. Allen J. Photoplethysmography and its application in clinical physiological measurement. Physiol Meas 2007;28:R1-39.
2. Safar ME. Arterial aging--hemodynamic changes and therapeutic options. Nat Rev Cardiol 2010;7:442-9.
3. Bosetti F, Galis ZS, Bynoe MS, Charette M, Cipolla MJ, Del Zoppo GJ, Gould D, Hatsukami TS, Jones TL, Koenig JI, Lutty GA, Maric-Bilkan C, Stevens T, Tolunay HE, Koroshetz W; "Small Blood Vessels: Big Health Problems" Workshop Participants. "Small Blood Vessels: Big Health Problems?": Scientific Recommendations of the National Institutes of Health Workshop. J Am Heart Assoc 2016;5:e004389.
4. Millasseau SC, Kelly RP, Ritter JM, Chowienczyk PJ. Determination of age-related increases in large artery stiffness by digital pulse contour analysis. Clin Sci (Lond) 2002;103:371-7.
5. Murray WB, Foster PA. The peripheral pulse wave: information overlooked. J Clin Monit 1996;12:365-77.
6. Allen J, Murray A. Age-related changes in peripheral pulse timing characteristics at the ears, fingers and toes. J Hum Hypertens 2002;16:711-7.
7. Allen J, Murray A. Modelling the relationship between peripheral blood pressure and blood volume pulses using linear and neural network system identification techniques. Physiol Meas 1999;20:287-301.
8. Hartmann V, Liu H, Chen F, Qiu Q, Hughes S, Zheng

D. Quantitative Comparison of Photoplethysmographic Waveform Characteristics: Effect of Measurement Site. Front Physiol 2019;10:198.

9. Tomlins PH, Wang RK. Theory, developments and applications of optical coherence tomography. J Phys D Appl Phys 2005;38:2519-35.

10. Wang RK, An L, Francis P, Wilson DJ. Depth-resolved imaging of capillary networks in retina and choroid using ultrahigh sensitive optical microangiography. Opt Lett 2010;35:1467-9.

11. An L, Qin J, Wang RK. Ultrahigh sensitive optical microangiography for in vivo imaging of microcirculations within human skin tissue beds. Opt Express 2010;18:8220-8.

12. Zhang A, Zhang Q, Chen CL, Wang RK. Methods and algorithms for optical coherence tomography-based angiography: a review and comparison. J Biomed Opt 2015;20:100901.

13. Chen CL, Wang RK. Optical coherence tomography based angiography [Invited]. Biomed Opt Express 2017;8:1056-82.

14. Wang RK. Optical Microangiography: A Label Free 3D Imaging Technology to Visualize and Quantify Blood Circulations within Tissue Beds in vivo. IEEE J Sel Top Quantum Electron 2010;16:545-54.

15. Yousefi S, Zhi Z, Wang RK. Eigendecomposition-based clutter filtering technique for optical micro-angiography. IEEE Trans Biomed Eng 2011;58:10.1109/TBME.2011.2152839.

16. Zhang Q, Wang J, Wang RK. Highly efficient eigen decomposition based statistical optical microangiography. Quant Imaging Med Surg 2016;6:557-63.

17. Wang RK, Zhang Q, Li Y, Song S. Optical coherence tomography angiography-based capillary velocimetry. J Biomed Opt 2017;22:66008.

18. Yousefi S, Wang RK. Simultaneous estimation of bidirectional particle flow and relative flux using MUSIC-OCT: phantom studies. Phys Med Biol 2014;59:6693-708.

19. Yousefi S, Qin J, Wang RK. Super-resolution spectral estimation of optical micro-angiography for quantifying blood flow within microcirculatory tissue beds in vivo. Biomed Opt Express 2013;4:1214-28.

20. Lai N, Saidel GM, Iorio M, Cabrera ME. Non-invasive estimation of metabolic flux and blood flow in working muscle: effect of blood-tissue distribution. Adv Exp Med Biol 2009;645:155-60.

21. Reisner A, Shaltis PA, McCombie D, Asada HH. Utility of the photoplethysmogram in circulatory monitoring.

Anesthesiology 2008;108:950-8.

22. Bahadir Z, Tisdell E, Arce Esquivel AA, Dobrosielski DA, Welsch MA. Influence of venous emptying on the reactive hyperemic blood flow response. Dyn Med 2007;6:3.

23. Hickey M, Phillips JP, Kyriacou PA. The effect of vascular changes on the photoplethysmographic signal at different hand elevations. Physiol Meas 2015;36:425-40.

24. Hickey M, Phillips JP, Kyriacou PA. Investigation of peripheral photoplethysmographic morphology changes induced during a hand-elevation study. J Clin Monit Comput 2016;30:727-36.

25. Almond NE, Jones DP, Cooke ED. Noninvasive measurement of the human peripheral circulation: relationship between laser Doppler flowmeter and photoplethysmograph signals from the finger. Angiology 1988;39:819-29.

26. Netea RT, Lenders JW, Smits P, Thien T. Both body and arm position significantly influence blood pressure measurement. J Hum Hypertens 2003;17:459-62.

27. Kamshilin AA, Krasnikova TV, Volynsky MA, Miridonov SV, Mamontov OV. Alterations of blood pulsations parameters in carotid basin due to body position change. Sci Rep 2018;8:13663.

28. Song S, Xu J, Men S, Shen TT, Wang RK. Robust numerical phase stabilization for long-range swept-source optical coherence tomography. J Biophotonics 2017;10:1398-410.

29. Braverman IM. The cutaneous microcirculation. J Investig Dermatol Symp Proc 2000;5:3-9.

30. Zhang A, Zhang Q, Wang RK. Minimizing projection artifacts for accurate presentation of choroidal neovascularization in OCT micro-angiography. Biomed Opt Express 2015;6:4130-43.

31. Zhang Q, Zhang A, Lee CS, Lee AY, Rezaei KA, Roisman L, Miller A, Zheng F, Gregori G, Durbin MK, An L, Stetson PF, Rosenfeld PJ, Wang RK. Projection artifact removal improves visualization and quantitation of macular neovascularization imaged by optical coherence tomography angiography. Ophthalmol Retina 2017;1:124-36.

32. Laughlin MH, Davis MJ, Secher NH, van Lieshout JJ, Arce-Esquivel AA, Simmons GH, Bender SB, Padilla J, Bache RJ, Merkus D, Duncker DJ. Peripheral circulation. Compr Physiol 2012;2:321-447.

33. Joyner MJ, Dietz NM, Shepherd JT. From Belfast to Mayo and beyond: the use and future of plethysmography to study blood flow in human limbs. J Appl Physiol (1985) 2001;91:2431-41.

34. Levick JR, Michel CC. The effects of position and skin temperature on the capillary pressures in the fingers and toes. J Physiol 1978;274:97-109.
35. Angius G, Barcellona D, Cauli E, Meloni L, Raffo L, Myocardial infarction and Antiphospholipid Syndrome: A first study on finger PPG waveforms effects. Krakow: 2012 Computing in Cardiology, 2012:517-20.
36. Wang A, Yang L, Liu C, Cui J, Li Y, Yang X, Zhang S, Zheng D. Athletic differences in the characteristics of the photoplethysmographic pulse shape: effect of maximal oxygen uptake and maximal muscular voluntary

37. Xiao MX, Wei HC, Xu YJ, Wu HT, Sun CK. Combination of R-R interval and crest time in assessing complexity using multiscale cross-approximate entropy in normal and diabetic subjects. Entropy 2018;20:497.
38. Burkert A, Scholze A, Tepel M. Noninvasive continuous monitoring of digital pulse waves during hemodialysis. ASAIO J 2006;52:174-9.
39. Millasseau SC, Ritter JM, Takazawa K, Chowienczyk PJ. Contour analysis of the photoplethysmographic pulse measured at the finger. J Hypertens 2006;24:1449-56.

contraction. Biomed Res Int 2015;2015:752570.